# Lanthanide containing compounds for therapeutic care in bone resorption disorders†‡§

**Cheri A. Barta,[a] Kristina Sachs-Barrable,[b] Jessica Jia,[b] Katherine H. Thompson,[a] Kishor M. Wasan*[b] and Chris Orvig*[a]**

***Received 4th April 2007, Accepted 31st May 2007***
***First published as an Advance Article on the web 11th September 2007***
**DOI: 10.1039/b705123a**



Lanthanide ions, Ln(III), are known functional mimics of Ca(II) ions and have been shown to affect the bone remodeling cycle. Exploiting this disruption to the bone remodeling cycle has potential for the treatment of bone density disorders, such as osteoporosis. In an effort to find new orally active agents for these disorders, a series of Ln(III) containing complexes incorporating small, non-toxic, bidentate pyrone and pyridinone ligands have been synthesized and characterized ($LnL_3$, Ln = La, Eu, Gd, Tb, Yb, L = 3-oxy-2-methyl-4-pyrone ($ma^-$), 3-oxy-2-ethyl-4-pyrone ($ema^-$), 3-oxy-1,2-dimethyl-4-pyridinone ($dpp^-$) and 3-oxy-2-methyl-4(1*H*)-pyridinone ($mpp^-$)). Preliminary biological analysis included cytotoxicity, cell uptake and bidirectional transport studies in Caco-2 cells and *in vitro* hydroxyapatite (HA) binding studies. The proportion of intact compounds bound to HA was calculated based on determination of Ln(III) concentration by ICP-MS and by UV-vis spectrophotometric assay of the proligand in solution. The $LnL_3$ species were found to have $IC_{50}$ values at least 6 times greater than that of cisplatin, ≥ 98% HA-binding capacity, and permeability coefficients in the moderate range. $La(dpp)_3$ was ascertained to be the lead compound for the treatment of bone density disorders with the highest percentage cell uptake of 9.07 ± 2.33% and the highest preliminary $P_{app}$ value of 3.54 ± 2.86 × $10^{-6}$ cm $s^{-1}$ compared to the other $LnL_3$ complexes tested.

## Introduction

Bone density disorders, including osteoporosis, affect 1 in 4 women and 1 in 8 men over age 50 in North America.[1] As the population ages, these diseases are incurring substantial annual health care costs escalating into billions of dollars. Osteoporosis is characterized by low bone mineral density that leads to enhanced bone fragility and a consequent risk of low-impact bone fractures.[2,3] The low bone mineral density is a result of an imbalance between bone resorption and bone formation. Normally, building and absorption of bone is a tightly regulated cycle wherein the bone matrix is manufactured by osteoblast cells and removed by osteoclast cells. Either increased activity of osteoclasts or decreased bone formation by osteoblasts leads to microarchitectural deterioration of bone tissue. Many contributing factors are known to influence the pathogenesis of the disease with the most prominent being inadequate calcium uptake.[2] Few therapeutic agents exist currently, either for prevention or for amelioration of these serious diseases.[2,4,5] In addition, patient compliance with the existing treatments is low due to adverse gastrointestinal side effects and, in the case of calcitonin, high costs.[2,4,5] A new class of osteoporosis drugs, including oral strontium ranelate, stimulate osteoblast proliferation and inhibit osteoclast activity,[6,7] however, uncertainty regarding the potential toxicity of chronic strontium accumulation in bone may limit the utility of this product.[8]

Low doses of Ln(III) have been shown to act similarly to strontium ranelate.[9–11] Lanthanides (Ln), the fourteen elements from cerium to lutetium (Ce–Lu, $Z$ = 58–71), are known for their therapeutic and diagnostic applications as agents for magnetic resonance imaging,[12] cancer,[13] luminescent labeling of biomolecules,[14] and radiotherapy.[15–17] Lanthanum (La, $Z$ = 57), although technically not a Ln, has many of the same characteristics of lanthanides and will be considered herein as a Ln. *In vivo*, Ln(III), a functional mimic of Ca(II),[15] has been found to exchange with Ca(II) in bone[9] and modify the bone remodeling cycle by stimulating osteoblast proliferation[10,11] and impeding bone resorption by inhibiting osteoclast differentiation.[11] Based on this evidence, lanthanum carbonate ($La_2(CO_3)_3$) has been proposed as a potential preventative measure for post-menopausal osteoporosis, however, gastrointestinal upset is a known negative side effect of this treatment.[9,11]

$La_2(CO_3)_3$ is currently being used to treat hyperphosphatemia under the trade name of Fosrenol™. Unfortunately, the extremely low bioavailability (<0.0007%) of Fosrenol™ requires that high doses of elemental La(III) be administered to control phosphate levels. The high doses of La(III) lead to adverse gastrointestinal (GI) tract side effects, with consequent poor patient compliance.[9]

Adjustments to the ligand structure around the Ln(III) ions have the potential to increase the oral bioavailability of Ln(III)

[a]*Medicinal Inorganic Chemistry Group, Department of Chemistry, University of British Columbia, 2036 Main Mall, Vancouver, British Columbia, V6T 1Z1, Canada. E-mail: orvig@chem.ubc.ca*
[b]*Faculty of Pharmaceutical Sciences, University of British Columbia, 2146 East Mall, Vancouver, BC, V6T 1Z3, Canada. E-mail: kwasan@interchange.ubc.ca*

† Based on the presentation given at Dalton Discussion No. 10, 3rd–5th September 2007, University of Durham, Durham, UK.

‡ The HTML version of this article has been enhanced with colour images.

§ Electronic supplementary information (ESI) available: Table of IR data and $^1$H NMR example of metal binding (Hma and $La(ma)_3$ spectrum). See DOI: 10.1039/b705123a

for the treatment of bone density disorders while decreasing unwanted side effects. Hydroxypyrones and hydroxypyridinones, related classes of small, bidentate, *O*,*O* proligands, exhibit high bioavailability and favorable toxicity profiles. Consisting of a 6-membered O or N heterocycle, respectively, these proligands form thermodynamically stable five membered chelate rings using the hard hydroxyl O atom and the neighboring ketone functionality. Upon deprotonation within the physiological pH range, both hydroxypyrones and hydroxypyridinones form neutral, stable (mostly tris) complexes with trivalent cations including $Fe^{3+}$, $Al^{3+}$, $Ga^{3+}$, $In^{3+}$,[18] and Ln(III),[19–21] as well as the actinides[22] and several divalent ions including $Zn^{2+}$, $Ru^{2+}$, $[VO]^{2+}$, and $[MoO_2]^{2+}$.[23] A handful of these metal complexes and their corresponding hydroxypyrone and hydroxypyridinone proligands have been extensively investigated for a myriad of potential biological applications including iron overload disorders,[24,25] aluminium toxicity,[26,27] orally active cancer treatments,[28] radiotherapeutic agents and use in SPECT imaging,[29–31] restoration of iron balance in anemia patients,[32–34] insulin-enhancing agents,[35] and Gd MRI contrast agents.[23,36]

Specific proligands of interest include maltol (Hma, 3-hydroxy-2-methyl-4-pyrone), its analogue ethylmaltol (Hema, 3-hydroxy-2-ethyl-4-pyrone), deferiprone (Hdpp, 3-hydroxy-1,2-dimethyl-4-pyridinone), and 3-hydroxy-2-methyl-4(1*H*)-pyridinone (Hmpp) (Scheme 1).[37] Hmpp, the only non-commercially available proligand used in this study, is synthesized in moderate yields by ammonolysis of a benzyl-protected maltol followed by acid deprotection.[38] Hydroxypyridinones are known to be significantly stronger chelators than are their hydroxypyrone analogues allowing the stability of the complexes to be tuned by switching the ligand or the metal to obtain desired properties.[25]

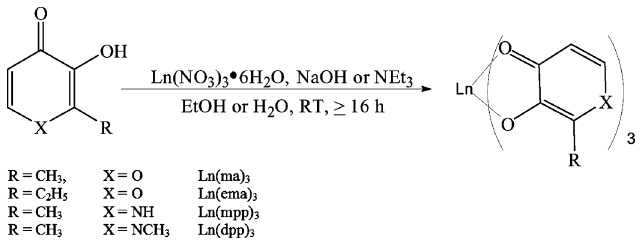


**Scheme 1** 3-Hydroxy-4-pyrones and 3-hydroxy-4-pyridinones of interest and their Ln complexes (Ln = La, Eu, Gd, Tb, Yb).

Previously, a handful of Ln(III) complexes using the same pyrone and pyridinone ligands have been investigated, including $Ln(ma)_3$ Ln = Pr, Nd, Sm, Gd, Dy, Yb, $Gd(ema)_3$ and $Gd(dpp)_3$;[39–41] however, these complexes have neither been fully characterized, nor have their potential utilities as bone density agents been investigated.

Herein, the synthesis and complete characterization of the neutral Ln(III) tris(bidentate ligand) complexes using Hma, Hema, Hmpp, and Hdpp as the ligands is presented. La(III), Gd(III), and Yb(III) ions were investigated, with selection of specific lanthanides based on their known medicinal applications and for size comparison. The luminescent properties of the Eu(III) and Dy(III) complexes were also studied. In addition, the potential of these compounds as therapeutic agents for the treatment of bone resorption disorders was assessed in cytotoxicity studies, comparative bifunctional transport studies in human colon carcinoma cells with intestinal cell-like properties (Caco-2 cells),[41–44] and hydroxyapatite binding assays.

## Results and discussion

### Metal complexes

The neutral $LnL_3$ where $L = ma^-$, $ema^-$, $mpp^-$, or $dpp^-$ complexes were synthesized using simple procedures (Scheme 1).[39–41,45–48] Due to the tendency of Ln(III) ions to hydrolyse easily with increasing pH, extreme care was taken when adjusting the pH of the solution. The complexes precipitated from the respective reaction mixtures to afford white or off-white air stable powders in moderate to high yields, with the exception of the Eu(III) complexes which precipitated as yellow powders. Attempts to recrystallize the complexes (in hot MeOH or EtOH) resulted, unfortunately, in decomposition of the product and hydrolysis of the Ln(III) ions. Column chromatography was useless for purification of the compounds due to their low solubilities. However, washing the precipitated solid thoroughly with cold solvents to remove unreacted ligand, additional $Ln(NO_3)_3$ salts or other side products yielded complexes pure by elemental analysis (Table 1). The compounds were thoroughly characterized by elemental analysis (EA), positive ion electrospray ionization-mass spectrometry (+ESI-MS), IR, and NMR ($LaL_3$). IR, EA and +ESI-MS results are all consistent with the formation of neutral $LnL_3$ species.

The IR spectra for all the complexes were dominated by peaks corresponding to the ligand (see Table S1 in ESI§);[39,49,50] however, the IR spectra for $LnL_3$ were nearly superimposable within each ligand set (<10 $cm^{-1}$ variations between Ln(III) ions with the same ligand, attributed to mass differences amongst the metal ions), indicating that the $Ln(ma)_3$, $Ln(ema)_3$, $Ln(mpp)_3$, and $Ln(dpp)_3$, regardless of the Ln(III) ion, are isostructural in the solid state. The $\nu_{C=O}$ stretching bands were shifted 40–50 $cm^{-1}$ to lower energy with respect to the proligand, evincing normal coordination of the metal *via* the ketonic oxygen and the oxygen of the deprotonated phenol group. The broad band for $\nu_{OH}$ disappeared upon complexation indicating complete deprotonation of the phenol OH group. New bands at 3400 and 3200 $cm^{-1}$ appeared for the pyrone and pyridinone complexes, respectively, due to lattice and coordinated water molecules. Resonance of the coordinated aromatic bidentate ligands resulted in a hyperchromic shift observed for $\nu_{C-O}$ due to the increasing double bond character of the C–O linkage. In addition, the $\nu_{C=C}$ vibrational modes were bathochromically shifted indicating a decrease in the double bond character of the aromatic ring due to donation of π electrons to the chelate ring. This trend is similarly seen in Ln(ONO) systems.[51] The absence of $\nu_{NO3}$ (~1382) in the IR spectra indicated the absence of any counterions in the complexes and the appearance of new peaks between 400–500 $cm^{-1}$ for $\nu_{M-O}$ stretching frequencies confirmed the complexation of ligands to their respective metal ions.[52,53]

The elemental analyses for all the lanthanide complexes confirmed the empirical formula $LnL_3 \cdot xH_2O$. Hydrated species have been observed with the previously synthesized $Ln(ma)_3$ and $Gd(ema)_3$ systems, in which at least one water molecule was associated with the metal compounds (Table 1).[39,40] In addition, the N–H functionality of the $mpp^-$ ligand is a potential hydrogen bond donor that may increase hydration numbers for its complexes.

 

**Table 1** Elemental analysis, % yield and +ESI-MS results for all prepared $LnL_3$ complexes

| Complex | %C found (calc) | %H found (calc) | %N found (calc) | % yield | $[NaLnL_3]^+$ |
|---|---|---|---|---|---|
| $La(ma)_3$ | 42.04 (42.40) | 2.94 (3.20) | | 40 | 537 |
| $Eu(ma)_3 \cdot H_2O$ | 39.65 (39.57) | 3.14 (3.32) | | 62 | 551 |
| $Gd(ma)_3 \cdot H_2O$ | 39.27 (39.28) | 3.11 (3.11) | | 59 | 556 |
| $Tb(ma)_3 \cdot H_2O$ | 39.15 (38.87) | 3.10 (3.04) | | 54 | 557 |
| $Yb(ma)_3$ | 39.43 (39.43) | 2.76 (3.10) | | 36 | 571 |
| $La(ema)_3$ | 45.34 (45.74) | 3.80 (4.14) | | 68 | 579 |
| $Eu(ema)_3 \cdot 2.5H_2O$ | 41.02 (41.05) | 3.94 (4.27) | | 64 | 593 |
| $Gd(ema)_3$ | 43.89 (44.18) | 3.68 (3.97) | | 53 | 598 |
| $Tb(ema)_3 \cdot H_2O$ | 42.44 (42.61) | 3.90 (3.91) | | 56 | 599 |
| $Yb(ema)_3$ | 42.72 (42.32) | 3.58 (3.89) | | 85 | 614 |
| $La(mpp)_3 \cdot 2H_2O$ | 36.33 (36.06) | 4.94 (4.71) | 6.05 (6.12) | 52 | 534 |
| $Eu(mpp)_3 \cdot 2H_2O$ | 38.58 (38.63) | 3.96 (3.68) | 7.50 (7.87) | 46 | 547 |
| $Gd(mpp)_3$ | 40.82 (40.49) | 3.43 (3.82) | 7.93 (8.06) | 38 | 553 |
| $Tb(mpp)_3 \cdot 2H_2O$ | 38.11 (37.80) | 3.91 (3.71) | 7.41 (7.62) | 56 | 554 |
| $Yb(mpp)_3$ | 42.93 (42.78) | 4.12 (3.89) | 7.15 (6.92) | 64 | 568 |
| $La(dpp)_3$ | 45.58 (45.95) | 4.37 (4.74) | 7.59 (7.82) | 40 | 576 |
| $Eu(dpp)_3 \cdot H_2O$ | 43.16 (43.18) | 4.48 (4.82) | 7.19 (7.18) | 38 | 590 |
| $Gd(dpp)_3 \cdot H_2O$ | 42.77 (42.76) | 4.44 (4.67) | 7.13 (7.04) | 76 | 595 |
| $Tb(dpp)_3 \cdot 2H_2O$ | 41.39 (41.67) | 4.63 (4.88) | 6.90 (7.03) | 54 | 596 |
| $Yb(dpp)_3 \cdot 3H_2O$ | 39.32 (39.25) | 4.71 (4.54) | 6.55 (6.82) | 68 | 610 |



Electrospray ionization mass spectrometry in the positive ion mode gave diagnostic mass spectra with the expected isotopic patterns. The most intense peak corresponded to the sodium adduct of the parent ion peak $[NaLnL_3]^+$ (Table 1). Peaks corresponding to $[LnL_2]^+$ species generated by the gas-phase loss of one ligand were observed in addition to peaks with the formula $[Ln_2L_5]^+$, as commonly reported for other trivalent metal-tris(*O*,*O* bidentate ligand) analogues.[47,54]

The literature crystal structure of $Pr(ma)_3$ revealed three bidentate deprotonated coordinated ligands and two bound water molecules arranged in an irregular geometry around the Pr(III) ion,[41] matching perfectly the analytical data obtained in this study. In addition, the C–O bond distances of the donor oxygens were not significantly different, suggesting that the negative charge is delocalized upon coordination, as would be expected in the reported complexes.

The NMR spectra of $LaL_3$ were also useful in elucidating the structure of the metal complexes. All diamagnetic $LaL_3$ were studied in solution by $^1$H NMR (Table 2 and Fig. 1S in ESI§). Only $La(ma)_3$ and $La(ema)_3$ were analyzed by $^{13}$C NMR due to limited solubility of the pyridinone complexes (Table 3). The absence of ligand peaks and the relative shifts in both the $^1$H and $^{13}$C NMR signals conclusively indicated binding of the ligand to the $La^{3+}$ ion. Both ring hydrogens, $H_a$ and $H_b$, for the La(III) pyrone and pyridinone metal complexes shifted upfield. Similar upfield shifts were reported in the corresponding Ln(III) complexes with the pyridinethiones and pyronethiones as ligands.[46]

**Table 2** $^1$H NMR data for La(III) complexes (300 MHz, RT, DMSO-$d_6$, X = O for Hma, Hema, $La(ma)_3$ and $La(ema)_3$, NH for Hmpp, $La(mpp)_3$ and $NCH_3$ for Hdpp, $La(dpp)_3$). Coupling constants are listed in parentheses.

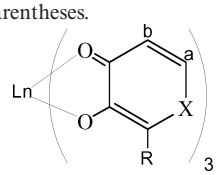


3

| Compound | R[a] | $H_a$(d) | $H_b$(d) | OH |
|---|---|---|---|---|
| Hma | 2.23 | 8.00 ($^3J$ = 5.4) | 6.33 ($^3J$ = 5.4) | 8.80 |
| $La(ma)_3$ | 2.20 | 7.93 ($^3J$ = 5.0) | 6.23 ($^3J$ = 3.1) | |
| Hema | 2.61<br>1.09 ($^3J$ = 7.3) | 8.01 ($^3J$ = 4.6) | 6.33 ($^3J$ = 5.4) | 8.79 |
| $La(ema)_3$ | 2.57<br>1.00 ($^3J$ = 7.3) | 7.90 ($^3J$ = 5.0) | 6.16 ($^3J$ = 4.6) | |
| Hmpp | 2.17 | 7.39 ($^3J$ = 6.9) | 6.09 ($^3J$ = 6.9) | 8.31 |
| $La(mpp)_3$[b] | 2.15 | 7.26 (br = 0.3 ppm) | 6.07 (br = 0.3 ppm) | |
| Hdpp | 2.25<br>3.62[c] | 7.54 ($^3J$ = 7.31) | 6.07 ($^3J$ = 6.85) | 8.31 |
| $La(dpp)_3$[b] | 2.26<br>3.63[c] | 7.47 (br = 0.35 ppm) | 6.03 (br = 0.35 ppm) | |

[a] R = $CH_3$ (s) for Hma, Hmpp, Hdpp, $La(ma)_3$, $La(mpp)_3$, $La(dpp)_3$; R = $CH_2$ (q) $CH_3$ (t) for Hema and $La(ema)_3$ [b] The coupling constants for the aromatic protons could not be calculated due to broad peaks instead of defined doublets seen for the proligands. [c] $\delta$ of the $-NCH_3$ moiety of Hdpp, $La(dpp)_3$; abbreviations: s = singlet, d = doublet, t = triplet, q = quartet.

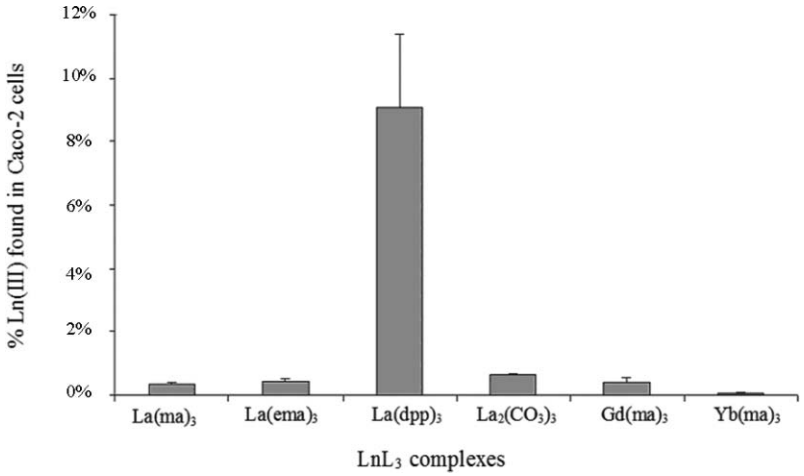


**Fig. 1** Cell uptake of $LnL_3$ in Caco-2 cells determined by ICP-MS. Values are presented as a mean percentage of Ln(III) added g protein$^{-1}$ well$^{-1}$ ± SD, $n = 6$. $La(dpp)_3$ exhibits significantly higher cell uptake ($P < 0.001$).

**Table 3** $^{13}C$ NMR data for the La(III) pyrone complexes (300 MHz, RT, DMSO-$d_6$).

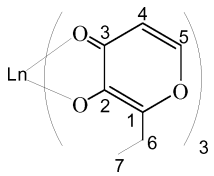


| Cmpd | C1 | C2 | C3 | C4 | C5 | C6[a] | C7 |
|---|---|---|---|---|---|---|---|
| Hma | 149.97 | 149.23 | 172.56 | 113.56 | 154.62 | 13.94 | |
| $La(ma)_3$ | 149.27 | 154.15 | 180.10 | 111.16 | 152.54 | 14.30 | |
| Hema | 154.81 | 153.39 | 172.90 | 113.52 | 142.39 | 21.09 | 10.88 |
| $La(ema)_3$ | 153.46 | 168.26 | 181.00 | 110.86 | 152.07 | 20.54 | 11.12 |

[a] C6 is $CH_3$ group for Hma and $Ln(ma)_3$

A larger upfield shift was seen for $H_b$ ($\Delta\delta$ ~0.10–0.17 ppm) than for $H_a$ ($\Delta\delta$ ~0.07–0.11 ppm) on the La(III) pyrone ligands, whereas a larger shift for $H_a$ ($\Delta\delta$ ~0.13–0.07 ppm) compared to $H_b$ ($\Delta\delta$ ~0.02–0.04 ppm) was seen in the La(III) pyridinone ligands. This difference in the shifts of the La(III) pyrone and pyridinone ligands can be attributed to the increased electron density in the pyridinone ligands donated from the ring N atom. The nitrogen atom stabilizes the pyridinone complex by adding electron density to the ring current of the ligand from its lone pair of electrons. The chemical shifts of the methyl and ethyl groups on the ligands remain almost unchanged. In addition, there is only one set of broad peaks assigned to the ring hydrogens on the ligands, suggesting that their chemical shifts are either averaged values from the rapidly interconverting optical (Δ and Λ) and geometric (*facial* and *meridional*) isomers at RT, or due to the presence of water molecules in the coordination sphere.[54]

In the $^{13}C$ NMR spectra of $La(ma)_3$ and $La(ema)_3$, the most significant chemical shifts were observed for the C=O ($\Delta\delta$ ~7.54–8.10 ppm) and C–O–La ($\Delta\delta$ ~4.92–14.87 ppm) consistent with the La(III) ions being bound to the ligand through the *O*,*O* moiety. Both these signals were shifted downfield due to donation of electron density from the binding moieties to the metal ion. Peaks representing the other carbons in the ring, C1, C4, and C5 shifted upfield, with the biggest shifts seen for the C4 and C5 carbons ($\Delta\delta$ ~2.08–9.28 ppm). The $^{13}C$ NMR signals from the methyl group of $La(ma)_3$ or from the ethyl group of $La(ema)_3$ did not shift significantly ($\Delta\delta$ ~0.24–0.55 ppm). The broadening of the carbon signals also suggested the presence of isomers at RT.

The unique electronic properties of lanthanide cations, particularly Tb(III) and Eu(III), (long luminescent lifetimes, sharp emission bands, and large energy gap between absorbance and emission band of complexes) render these metal centers attractive for luminescence studies.[55,56] Unfortunately, the extinction coefficients for lanthanide ions tend to be small, however, this can be easily corrected by utilizing sensitized luminescence with radiationless energy transfer from an aryl chromophore to the metal ion.[57,58] By using this 'antenna effect', the Ln(III) ion luminesces with increased intensity in the visible region.

The pyrone and pyridinone ligands can photosensitize Ln(III) luminescence due to their UV absorption and appreciable molar absorptivity coefficients.[51] Luminescent excited states of the Tb(III) and Eu(III) complexes were generated *via* excitation of the pyrone and pyridinone moieties using UV wavelengths ranging from 315–324 nm. Energy was transferred to the $^5D_4$ or $^5D_0$ excited states of the Tb(III) or Eu(III), respectively (Table 4). Their fluorescence

**Table 4** Fluorescence data for the Eu(III) and Tb(III) complexes ($\lambda$ in nm). The strongest emissions for the Eu(III) and Tb(III) complexes are from $^5D_0 \rightarrow {}^7F_2$ and $^5D_4 \rightarrow {}^7F_5$, respectively. All other emission peaks seen in the fluorescence spectra are listed

| Complex | $\lambda_{exc}$/nm | $^5D_0 \rightarrow {}^7F_2$ | $^5D_0 \rightarrow {}^7F_0$ | $^5D_0 \rightarrow {}^7F_1$ | Complex | $\lambda_{exc}$/nm | $^5D_4 \rightarrow {}^7F_5$ | $^5D_4 \rightarrow {}^7F_6$ | $^5D_4 \rightarrow {}^7F_4$ |
|---|---|---|---|---|---|---|---|---|---|
| $Eu(ma)_3$ | 319 | 642 | 618 | 704 | $Tb(ma)_3$ | 315 | 641 | 545 | 705 |
| $Eu(ema)_3$ | 320 | 639 | 617 | 703 | $Tb(ema)_3$ | 317 | 637 | 545 | 701 |
| $Eu(mpp)_3$ | 322 | 647 | | 713 | $Tb(mpp)_3$ | 324 | 651 | | 721 |
| $Eu(dpp)_3$ | 294 | 616 | | 682 | $Tb(dpp)_3$ | 309 | 620 | | 684 |



 

was red-shifted *ca.* 300 nm from the maximum absorbance through possible emission transition states $^7F_j$ $j = 6$–0 with the most intense peaks resulting from $^5D_4 \rightarrow {}^7F_5$ and $^5D_0 \rightarrow {}^7F_2$ transitions, respectively.[59,60] Most of the other transition states were not observed as they were weak or outside the fluorimeter detection wavelengths. The emission bands of the complexes were also red-shifted slightly from the spectra of the $Eu(NO_3)_3$ and $Tb(NO_3)_3$ starting materials, reflecting the substitution of water and nitrate ligands with the coordinating O atoms of the pyrones and pyridinones. Ligand emission was observed, suggesting incomplete ligand-to-lanthanide energy transfer. The intensity ratio for the hypersensitive $^5D_0 \rightarrow {}^7F_5$ transition and the magnetic dipole transition $^5D_0 \rightarrow {}^7F_1$ with a value of ~25, indicates the absence of imposed symmetry on the complex observed in the NMR data. Complexes with $^7F_2/{}^7F_1$ intensity ratio lower than 0.7 have centrosymmetric coordination spheres, whereas an intensity ratio higher than 8 is indicative of low symmetry environments.[61,62]

### Cellular toxicity and uptake studies

One of the limitations of Ln(III) ions is their inability to cross cell membranes, particularly intestinal barriers, as exemplified by the FDA approved $La_2(CO_3)_3$.[15,63] Masking the Ln(III) ion with ligands designed to form small, lipophilic, low molecular weight compounds, we aim to lower the dose and minimize unwanted side effects by increasing the selective bioavailability of the Ln(III) ions.

A Caco-2 cell assay was used as a model for the absorption and secretion of molecules crossing the intestinal membrane. Caco-2 cells, originally derived from a human colorectal carcinoma line, differentiate at confluency into highly functional epithelial barriers with morphological and biochemical similarities to the small-intestinal columnar epithelium.[42–44,49] These cells have been used to evaluate the relative bioavailability and transport mechanisms of diverse drugs *in vitro*.[64–68] When grown as a monolayer on a semipermeable membrane, the passage of drugs across the Caco-2 cell barrier can be monitored by analyzing the concentration of the desired compounds transported to either the basolateral (B, bottom) side through the mimicked intestinal environment, or to the apical (A, top) side through secretory transport. In addition, the concentrations of compounds present inside the cells can be measured by digesting the cell membrane to release the cytosol contents.

Inductively coupled plasma mass spectrometry, ICP-MS, was used to measure the bifunctional transport of the $LnL_3$ across the Caco-2 cell barrier, and the metal ion concentrations of the apical, basolateral, and cell membrane. Regarded as one of the best analytical tools for the quantitative determination of lanthanides, ICP-MS can detect Ln(III) ion concentrations $\leq 1$ ppt.[69] Unfortunately, this study does not allow us to determine the composition of the compound being transported, in the biological media, or in the cell. However, one can qualitatively determine if the metal complexes increase the bioavailability of Ln(III) ions across an intestinal barrier, compared to the benchmark compound, $La_2(CO_3)_3$.

MTT (3-(4,5-dimethylthiazol-2-yl)-2,5-diphenyl tetrazolium bromide) assays were used to evaluate the cytotoxicity of $Ln(ma)_3$, $Ln(ema)_3$, $Ln(mpp)_3$ and $Ln(dpp)_3$ complexes using Caco-2 cells (Table 5). This colorimetric assay, commonly used for the initial stages of drug screening, determines cell viability by measuring the mitochondrial activity of *in vitro* cell lines after the addition of selected compounds.[70] The NADPH or NADH produced by mitochondrial dehydrogenase enzymes reduces the tetrazolium salts to colored formazan crystals that can be measured spectrophotometrically. A low $IC_{50}$ implies cytoxity or antiproliferation of the cells at low drug concentrations.

**Table 5** Cytotoxicity data (MTT assay) for the $LnL_3$ complexes, $n \geq 6$ (±SD)

| Complex | $IC_{50}$/μM |
|---|---|
| cisplatin | 8.67 (0.26) |
| Hma | >800 |
| $La(ma)_3$ | 155.58 (8.58) |
| $Gd(ma)_3$ | 118.37 (9.16) |
| $Yb(ma)_3$ | 107.92 (4.46) |
| Hema | >714 |
| $La(ema)_3$ | 138.95 (18.05) |
| $Gd(ema)_3$ | 107.75 (4.42) |
| $Yb(ema)_3$ | 144.13 (25.11) |
| Hmpp | 451.7 (4.56) |
| $La(mpp)_3$ | 142.30 (6.18) |
| $Gd(mpp)_3$ | 136.1 (1.15) |
| $Yb(mpp)_3$ | 136.5 (4.67) |
| Hdpp | 719 |
| $La(dpp)_3$ | 161.72 (2.08) |
| $Gd(dpp)_3$ | 120.78 (16.05) |
| $Yb(dpp)_3$ | 70.47 (4.42) |

The metal complexes were considerably more toxic than the analogous proligands after incubation with the cells for 72 h, but less toxic than cisplatin, a known chemotherapeutic which has an $IC_{50} = 8.67 \pm 0.26$ μM in Caco-2 cells.[71] All $IC_{50}$ values were in the same range, independent of the particular bidentate ligand, with the lowest $IC_{50} = 70.47 \pm 4.42$ μM for $Yb(dpp)_3$ and the highest being $161.72 \pm 2.08$ μM for $La(dpp)_3$. A lack of differential toxicity for the various complexes was determined.

All compounds, including $La_2(CO_3)_3$ exhibited similar cell uptake independent of the particular ligand (0.26–0.65% uptake), with the exception of $La(dpp)_3$ that showed cell uptake of 9.07 ± 2.33% ($P < 0.001$, Fig. 1). Hdpp is the most lipophilic of the ligands used and lipophilicity may increase cell passage. Masking of the Ln(III) metal with the $dpp^-$ ligand resulted in a considerable increase in cellular uptake of elemental Ln(III) compared to $La_2(CO_3)_3$.

No reduction in the transepithelial electrical resistance (TEER) was observed during the bifunctional uptake studies indicating that the integrity of the monolayer of the Caco-2 cells was not disturbed at the concentrations of $LnL_3$ and time points tested. Slight differences in apparent permeability ($P_{app}$, cm $s^{-1}$) coefficients from A-to-B *vs.* B-to-A transport were found between compounds (Fig. 2). $Yb(ma)_3$ exhibited a lower $P_{app}$ value for both A–B and B–A compared to the other $LnL_3$ species. In contrast, $La(dpp)_3$, presumably the most stable of the complexes, showed a higher A–B uptake. However, the B-to-A $P_{app}$ value for $La(dpp)_3$ was not significantly different than the values for the other $LaL_3$ tested. When chelated to the Ln(III), the $P_{app}$ ($\times 10^{-6}$ cm $s^{-1}$) values were significantly lowered compared to the proligand, namely Hddp with previously reported $P_{app}$ values of $22.3 \pm 1.2 \times 10^{-6}$ cm $s^{-1}$and $18.5 \pm 0.8 \times 10^{-6}$ cm $s^{-1}$ for the A-to-B and B-to-A transport, respectively.[72] In any case, the $LnL_3$ species tested exhibit similar partition coefficients as other small

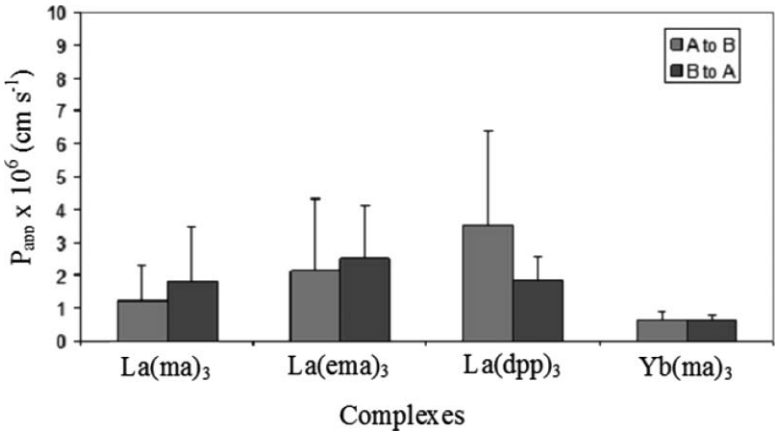


**Fig. 2** Apparent permeability ($P_{app}$) ± SD of La(ma)$_3$, La(ema)$_3$, La(dpp)$_3$ and Yb(ma)$_3$, across a Caco-2 membrane, $n = 6$. Both data sets, basolateral to apical (B → A) and apical to basolateral (A → B), were measured by ICP-MS after 4 h of exposure to $LnL_3$.



bioavailable drugs such as dopamine, a sympathetic nervous system agent (9.33 ± 3.48 cm $s^{-1}$), mannitol, used to reduce intracranial pressure (0.38 ± 0.12 cm $s^{-1}$), acebutalol hydrochloride, a cardiovascular agent (0.51 ± 0.02 cm $s^{-1}$), and Zidovudine, an antiretroviral drug for the treatment of HIV (6.93 ± 0.17 cm $s^{-1}$) as reported by other investigators.[65] In addition, one of our complexes has significantly greater bioavailability than does the benchmark $La_2(CO_3)_3$ based on preliminary results.

### *In vitro* hydroxyapatite binding studies

La(ma)$_3$, Tb(ma)$_3$, Gd(ma)$_3$, Eu(ma)$_3$, Yb(ma)$_3$, La(ema)$_3$, La(dpp)$_3$, and $La_2(CO_3)_3$ (tested at concentrations of 1 μM, well below their respective $IC_{50}$ values) showed high HA binding with a quantitative uptake of > 98% of the Ln(III) onto HA after 24 h incubation. Minimal variability was observed between lanthanides (Fig. 3). In addition, > 95% Ln(III) ions were adsorbed onto the HA in 5 min or less. La(dpp)$_3$, Gd(ma)$_3$ and Yb(ma)$_3$ had slightly slower binding kinetics, possibly due to the stability of the complexes. Yb(III) and Gd(III) ions are stronger Lewis acids than is the slightly larger La(III) ion. Thus, these ions bind more tightly to the hard *O*,*O* donors of the pyrone and pyridinone ligands further competing with the HA binding moieties. Stability of the complex may explain the slower uptake of La(dpp)$_3$ (95.8 ± 1.7% at 3 h) compared to the other $LaL_3$ complexes tested (99.1 ± 0.4% for La(ma)$_3$ and 99.81 ± 0.01% for La(ema)$_3$ at 3 h). Pyridinones are known to be stronger binders than are their pyrone analogs due to the ring N donating more electron density than its electronegative O counterpart.[23,73]

Fluorescence studies were used to determine quantitatively the amount of the Ln(III) ions unbound to HA by measuring the fluorescence of the supernatant from the Tb(ma)$_3$ and Eu(ma)$_3$ samples. The fluorescence results confirmed the ICP-MS data showing > 98% Ln–HA binding after 24 h ($P > 0.05$ compared to the $LnL_3$ species analyzed by ICP-MS, Fig. 3).

A colorimetric assay, with xylenol orange (sodium salt) dye indicative of free Ln(III) ions, was also used to confirm the ICP-MS results.[74–76] In acidic buffered solutions, xylenol orange reddens in the presence of free Ln(III) ions. In contrast, appearance of a yellow–orange colour indicates the absence of unbound Ln(III) ions. Solutions of proligand and HA were used as negative controls, solutions of $Ln(NO_3)_3$ served as positive controls. As expected, the proligands, HA and the $LnL_3$ solutions turned weakly yellowish–orange suggesting the absence of unbound Ln(III) in solution; however, the $Ln(NO_3)_3$ solution turned a dark red–purple.

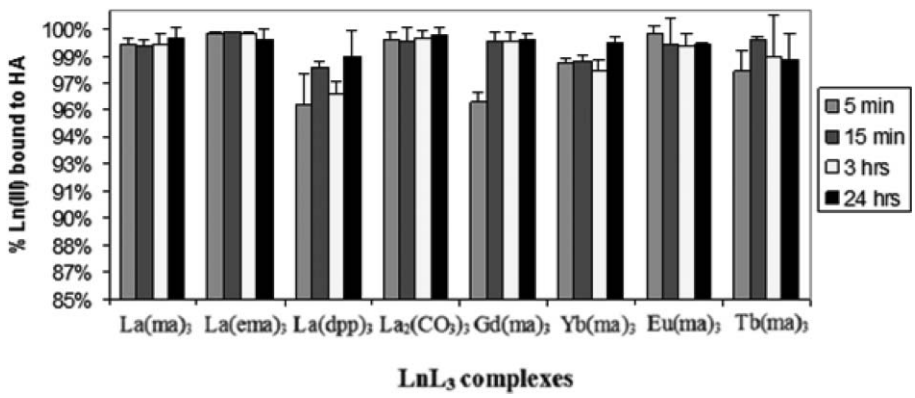


**Fig. 3** Percentage ± SD of Ln(III) bound to HA samples, $n = 6$. Tb(III) and Eu(III) concentrations were determined by measuring the fluorescence of the Tb(ma)$_3$ or Eu(ma)$_3$ species in the supernatant, respectively, and subtracting the amount found from the total amount of $LnL_3$ added. All other Ln(III) concentrations were determined by ICP-MS analysis ($P > 0.05$ between samples at 24 h).

 

Solid samples from the metal–HA binding studies as well as the supernatant from the same experiment were tested for the presence of free Ln(III) ions. The addition of acid was presumed to digest the hydroxyapatite of the solid sample thereby releasing any bound Ln(III) ions into solution. In concordance with the ICP-MS data, the supernatant turned a slightly darker orange–yellow than did the controls, suggesting a low concentration of free Ln(III). The digested Ln–HA samples turned dark red indicating an abundance of free Ln(III) ions. These results confirm the ICP-MS data indicating a large proportion of the Ln(III) ions present on the HA matrix.

To further confirm these results, xylenol orange was added to an undigested Ln–HA sample in the buffer solution. The solution remained yellow–orange, but the particles turned a dark red–purple suggesting the presence of Ln(III) ions on the surface of the HA solid samples.

Spectrophotometric determination (UV-vis assay) of ligand concentration in supernatants from $La(ma)_3$, $Eu(ma)_3$, $Gd(ma)_3$, $Tb(ma)_3$, $Yb(ma)_3$, $La(ema)_3$, and $La(dpp)_3$–HA binding studies indicated that at the 24 h time point, > 97% of the ligand remained in solution independent of the metal complex tested (Fig. 4). High concentration of the ligand in solution indicated disassociation of the $LnL_3$ complex suggesting that the bidentate ligands on the Ln(III) ion were almost completely replaced by the phosphates and carbonate of the HA matrix.

IR spectra of the solid HA samples exposed to the Ln(III) complexes were compared to spectra of pure HA, the proligand, and the HA-bound $LnL_3$ complexes (Fig. 5). Irrespective of the metal ion, the complex or the exposure time of the $LnL_3$ species to the solid HA, the IR spectra were nearly superimposable with that of pure HA suggesting that the HA composition had not been modified upon complexation of the Ln(III) salt.[77–80] Although not prominent, the hydroxyl stretching (–OH) and bending bands were observed at 3569 and 630 $cm^{-1}$ for the HA–Ln samples. Broad bands at 3450 and 1640 $cm^{-1}$ were attributed to adsorbed water. The $\nu_3$ and $\nu_1$ $PO_4^{3-}$ vibrations were assigned to broad bands at 1043 and 969 $cm^{-1}$, respectively. Bands at 602 and 567 $cm^{-1}$ were from the $\nu_4$ vibrations. The band observed at 877 $cm^{-1}$ corresponds to $HPO_4^{2-}$ vibrations. The $\nu_3$ bands of carbonate ions observed at 1460 and 1425 $cm^{-1}$ are generally representative of substitution of phosphate groups for carbonate species. A new peak observed at ~474 $cm^{-1}$ corresponds to $\nu_{Ln-O}$ vibrations showing that the Ln(III)

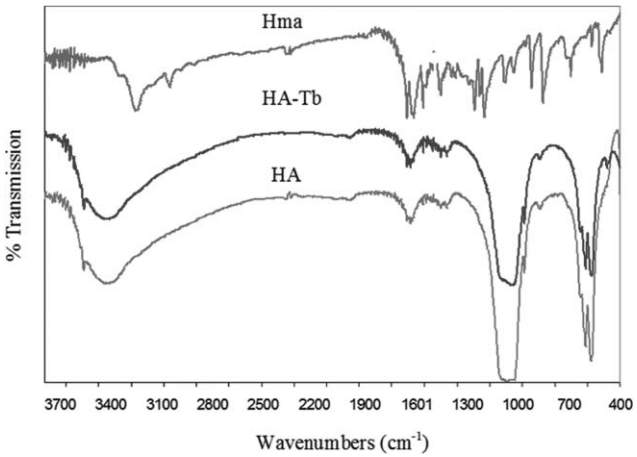


**Fig. 5** IR spectra from HA binding studies.

is bound to the HA upon coordinating to either the phosphate or the carbonate oxygens of the hydroxyapatite. In addition, vibrations from the proligand in the Ln–HA samples were not observed, consistently suggesting that the Ln(III) dissociates upon complexation to the HA.

The lack of IR shifts arising from the pure HA *versus* the Ln(III)–HA are not surprising due to the similarities of the Ca(II) and Ln(III) ions. Despite the slightly larger unit-cell volume found for Ln(III)–HA compared to Ca(II)–HA, Ln(III) are essentially functional mimics of Ca(II) ions sharing similar ionic radii, donor atom preferences, and almost identical coordination numbers in protein binding sites.[9,81]

## Summary

Twenty $LnL_3$ were successfully synthesized using Hma, Hema, Hmpp, or Hdpp as proligands. La(III), Gd(III), and Yb(III) complexes were chosen, in order to evaluate size affects and assess their medicinal applications, Tb(III) and Eu(III) complexes were of interest due to their characteristic fluorescence properties. Toxicity, bifunctional transport across a model of an intestinal barrier, and binding coefficients to HA were evaluated for several of the $LnL_3$ species to assess their potential therapeutic use for bone resorption disorders. By comparison with Fosrenol™, an FDA approved lanthanum-containing phosphate binder, the $LnL_3$ compounds

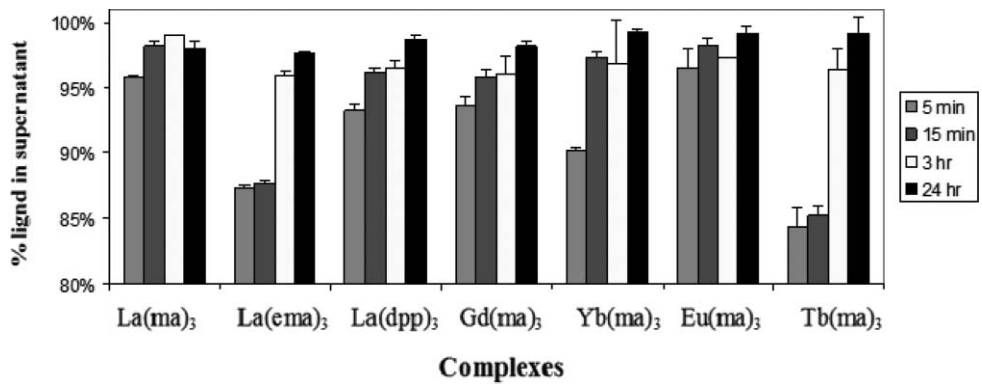


**Fig. 4** Percent ligand concentration ± SD remaining in the supernatant of the Ln(III)–HA binding studies determined by UV-vis spectroscopy ($P > 0.05$ between complexes at 24 h), $n = 6$.

investigated showed similar HA-binding (> 98%) and one of the compounds had greater absorption across an intestinal barrier, compared to lanthanum carbonate. The $LnL_3$ compounds were significantly less toxic than cisplatin and did not appear to disturb the HA structure upon binding. These novel $LnL_3$ thus have potential as orally available bone resorption inhibition drugs, with minimized side effects that may also serve as potential preventative supplements for osteoporosis. $La(dpp)_3$ was identified as the lead compound with high HA-binding (98.45 ± 1.45%) and a moderate $P_{app}$ value. This compound will be further tested in appropriate animal models of bone disorders for both bioavailability and anti-resorptive activity.

## Experimental

### Chemicals

NaOH, 3-hydroxy-1,2-methyl-4-pyridinone (Hdpp), hydrated lanthanum carbonate and hydrated lanthanide nitrate salts were obtained from Sigma-Aldrich, Fisher Scientific and Alfa Aesar and used without further purification. All solvents were reagent grade from Fisher Scientific. Maltol (Hma) and ethylmaltol (Hema) were obtained from Pfizer or Cultor Food Science. Water was deionized (Barnstead D8902 and D8904 Cartridges) and distilled (Hytrex II GX50-9-7/8 and GX100-9-7/8) before use. Water for HA studies and ICP-MS analysis was collected from Elgastat Prima 2 reverse osmosis and ultra pure water system (High Wycombe, England). NMR solvents were purchased from Aldrich and used as received. Yields for the analytically pure compounds were calculated based on the respective metal ion starting material.

### Instruments

$^1$H NMR spectra (300 MHz) and $^{13}$C NMR spectra (75 MHz) were recorded on a Bruker Varian XL-300 spectrometer and referenced internally to residual solvent protons. Infrared spectra were recorded as Nujol mulls (KBr windows) in the range 4000–500 $cm^{-1}$ on a Mattson Galaxy Series FTIR-5000 spectrophotometer and were referenced to polystyrene (1601 $cm^{-1}$). Analyses of C, H, and N were performed by Mr M. Lakha at the University of British Columbia. UV-visible spectra were recorded in water or 0.1% saline solution using a Hewlett-Packard 8543 diode array spectrophotometer and a 1 cm cuvette. Mass spectra were obtained on a Bruker Esquire Ion Trap (electrospray ionization mass spectrometry, ESIMS) spectrophotometer. Fluorescence spectra were obtained in 0.1% saline solution or methanol on a PTI QuantaMaster fluorimeter using a 1 cm quartz cuvette. A high resolution ICP-MS (Thermo Finnigan ELEMENT 2) was used for determination of metal ion concentration, calibrated against Delta Scientific Ltd. Standards.

**3-Benzyloxy-2-methyl-4-pyrone, Bnma.** This intermediate was prepared similarly to the previously published procedure with some modifications.[38] 3-Hydroxy-2-methyl-4-pyrone (5 g, 40 mmol) was dissolved in 200 mL of methanol and a solution of sodium hydroxide (3 g, 75 mmol in 30 mL of water) was added. After addition of benzyl chloride (7 mL, 61 mmol), the mixture was refluxed overnight and cooled in an ice bath. MeOH was removed from the yellow solution by rotary evaporation, 20 mL of additional water was added and the product was extracted into methylene chloride (2 × 20 mL). The water layer was discarded and the $CH_2Cl_2$ extracts were washed with 5% NaOH (3 × 15 mL), then water (1 × 20 mL). The $CH_2Cl_2$ layer was dried over $MgSO_4$, filtered, and the solvent was removed by rotary evaporation affording a viscous yellow oil. The oil was dissolved in hot ethanol and maintained at −5 °C for 48 h, after which time white cubic crystals formed. These were filtered out, washed with cold ethanol (3 × 5 mL), and vacuum dried (6.8 g, 31.5 mmol, 79% yield). $^1$H NMR (300 MHz, RT, $CDCl_3$) $\delta$ = 2.04 (s, 3H, $CH_3$), 5.10 (s, 2H, Bn–$CH_2$), 6.33 (d, 1H, $H_b$, $^3J_{b,a}$ = 5.1 Hz), 7.29 (m, 5H, Bn $C_6H_5$), 7.54 (d, 1H, $H_a$, $^3J_{a,b}$ = 5.6)

**3-Benzyloxy-2-methyl-4(1*H*)-pyridinone, Bnmpp.** Bnma (6.8 g, 31.5 mmol) in 80.5 mL of concentrated $NH_4OH$ and 30 mL of ethanol was stirred in a round bottomed flask at room temperature for 3 days. After each day, an additional 10 mL of ethanol was added. Ethanol and the excess ammonia were removed by rotary evaporation and the residue washed with 10 mL of acetone. The 3-benzyloxy-2-methyl-4(*1H*)-pyridone, Bnmpp, product was crystallized from ethanol as colorless crystals, filtered, and dried under vacuum overnight (4.3 g, 20.1 mmol, 64% yield). $^1$H NMR (300 MHz, RT, $CD_3OD$) $\delta$ = 2.05 (s, 3H, $CH_3$), 5.01 (s, 2H, Bn-$CH_2$), 6.34 (d, 1H, $H_b$, $^3J_{b,a}$ = 5.8 Hz), 7.31 (m, 5H, Bn $C_6H_5$), 7.86 (d, 1H, $H_a$, $^3J_{a,b}$ = 5.6)

**3-Hydroxy-2-methyl-4(1*H*)-pyridinone, Hmpp.** Bnmpp (4.3 g, 20.1 mmol) was debenzylated by treatment with 10 mL of 45% w/v hydrogen bromide–acetic acid solution for 30 min on a steam bath. Toluene by-product and excess solvent were removed by rotary evaporation. The precipitate was filtered out, redissolved in 10 mL of water and brought to pH 7–8 with the addition of 6 M NaOH. The solvent was removed by rotary evaporation. 3-Hydroxy-2-methyl-4(1*H*)-pyridinone (Hmpp) crystallized from ethanol as light pink crystals after 24 h in 4 °C (1.1 g, 8.64 mmol, 43%). $^1$H NMR (300 MHz, RT, $CD_3OD$) $\delta$ = 2.17 (s, 3H, $CH_3$), 6.09 (d, 1H, $H_b$, $^3J_{b,a}$ = 6.9 Hz), 7.39 (d, 1H, $H_a$, $^3J_{a,b}$ = 6.9), 8.31 (s, 1H, OH). MS (+ESI-MS, MeOH): *m/z* 126 $[M + H]^+$.

**General procedure for $Ln(ma)_3 \cdot nH_2O$, Ln = La, Eu, Gd, Tb, Yb.** $Ln(NO_3)_3 \cdot 6H_2O$ (0.433–0.467 g, 1.0 mmol) was added to a solution of Hma (0.378 g, 3.0 mmol) in 10 mL of deionized, distilled water and the solution was heated and stirred until the ligand completely dissolved (~10 min). The pH of the clear solution was raised slowly over 10 min with 1 M NaOH (Ln = La, pH 8.03; Eu, pH 8.00; Gd, pH 8.26; Tb, pH 8.5; Yb, pH 8.62) and the resulting reaction mixture was continuously stirred for 16 h. A white, or slightly off-white precipitate formed (except in the case of $Eu(ma)_3$ for which a yellow solid formed) and was collected by vacuum filtration, washed with 2 × 5 mL of cold water and 2 × 5 mL of cold MeOH. All compounds were dried *in vacuo* to yield 36–59% of product.

**General procedure for $Ln(ema)_3 \cdot nH_2O$, Ln = La, Eu, Gd, Tb, Yb.** $Ln(NO_3)_3 \cdot 6H_2O$ (0.433–0.467 g, 1.0 mmol) was added to a solution of Hema (0.420, 3.0 mmol) in 10 mL of ethanol and the solution was heated and stirred until the ligand completely dissolved (~5 min). Triethylamine (0.303 g, 3 mmol) was added slowly over 10 min to the clear solution. The resulting reaction mixture was continuously stirred for 18–24 h. A white or slightly off-white precipitate formed (except in the case of $Eu(ema)_3$ for

 

which a yellow solid formed) and was collected *via* vacuum filtration, washed with 2 × 5 mL of cold water and 2 × 5 mL of cold MeOH. All compounds were dried *in vacuo* to yield 53–85% of product.

**General procedure for Ln(dpp)$_3$·*n*H$_2$O, Ln = La, Eu, Gd, Tb, Yb.** Ln(NO$_3$)$_3$·6H$_2$O (0.433–0.467 g, 1.0 mmol) was added to a solution of Hdpp (0.417, 3.0 mmol) in 10 mL of deionized and distilled water and the solution was heated and stirred until the ligand completely dissolved (~30 min). The pH of the clear solution was raised slowly over 10 min with 6 M NaOH (Ln = La, pH 10.02; Eu, pH 10.20; Gd, pH 10.42; Tb, pH 11.00; Yb, pH 11.13) and the resulting reaction mixture was continuously stirred for 16 h. A white, or slightly off-white precipitate formed (except in the case of Eu(dpp)$_3$ for which a yellow solid formed) and was collected by vacuum filtration, washed with 2 × 5 mL of cold water and 2 × 5 mL of cold MeOH. All compounds were dried *in vacuo* to yield 40–76% of product.

**General procedure for Ln(mpp)$_3$·*n*H$_2$O, Ln = La, Eu, Gd, Tb, Yb.** Ln(NO$_3$)$_3$·6H$_2$O (0.144–0.154 g, 0.33 mmol) was added to a solution of Hmpp (0.125 g, 1.0 mmol) in 10 mL of deionized, distilled water and the solution was heated and stirred until the ligand completely dissolved (~30 min). The pH of the clear solution was raised slowly over 10 min with 6 M NaOH (Ln = La, pH 8.10; Eu, pH 8.20; Gd, pH 8.20; Tb, pH 8.30; Yb, pH 8.30) and the resulting reaction mixture was continuously stirred for 16 h. A white or slightly off-white precipitate formed (except in the case of Eu(mpp)$_3$ for which a yellow solid formed) and was collected by vacuum filtration, washed with 2 × 5 mL of cold water and 2 × 5 mL of cold MeOH. All compounds were dried *in vacuo* to yield 38–64% of product.

A complete list of compounds prepared and analytical data is presented in Table 1.

### Caco-2 cell culture

Caco-2 cells were purchased from American Type Culture Collection (ATCC, Rockville, MD and Manassas, VA, USA). Cell culture media were purchased from Gibco BRL (Grand Island, NY, USA). Sterile Steritop™ 0.22 μm Express membrane bottle top filters were purchased from Millipore (Bedford, MA, USA). Sterile 50 ml centrifuge tubes, disposable 10 and 25 mL serological pipettes were purchased from Starstedt (Montreal, PQ, Canada). Culture flasks, Transwell and polycarbonate plates were obtained from Corning-Costar (Cambridge, MA, USA). Triton X-100 was purchased from Sigma.

Caco-2 cells for MTT studies were cultured in 75 cm$^2$ Falcon tissue culture flasks in Eagle's Minimum Essential Medium (EMEM) supplemented with Eagle's BSS and 2 mM glutamine modified with 1.0 mM sodium pyruvate, 0.1 mM nonessential amino acids, 1.5 g L$^{-1}$ sodium bicarbonate and supplemented with 20% fetal bovine solution. The cells were incubated at 37 °C in a humidified atmosphere of 5% CO$_2$. Medium was changed every other day and the cell stock was routinely subcultured by trypsinization (0.25% trypsin with 0.53 mM EDTA) after reaching 80% confluency.

Caco-2 cells for cell uptake and transport studies were cultured in EMEM supplemented with 10% fetal bovine serum (FBS), 292 μg mL$^{-1}$ glutamine, 0.1 mM non-essential amino acids, 100 μg mL$^{-1}$ penicillin and 100 μg mL$^{-1}$ streptomycin at 37 °C in humidified air containing 5% CO$_2$ in either T75 flasks, 6-well, 12-well, 96-well or Transwell plates depending on the type of experiment. Medium was changed every other day. Cells used for experiments reached 80 to 90% confluency (in the case of transfer studies when the transepithelial electrical resistance (TEER) values were above 400 Ω cm$^2$, measured using Millicell-ERS from Millipore).

Data from cell permeability, cytotoxicity and hydroxyapatite binding (*vide infra*) studies were analyzed by ANOVA and Newman–Keuls post-analysis, where appropriate, and expressed as means ± SD. Studies were compared against La$_2$(CO$_3$)$_3$ unless otherwise stated. Statistical significance was accepted at $P < 0.05$.

### MTT assay

A modified procedure was used for the MTT assay (MTT = (3-(4,5-dimethylthiazol-2-yl)-2,5-diphenyltetrazolium bromide).[70] Caco-2 cells were seeded onto 96-well plates at a density of 1 × 10$^4$ cells per well. On the day of the experiment, the culture medium was exchanged for treatment solution of 1 μg mL$^{-1}$, 10 μg mL$^1$, 50 μg mL$^{-1}$, 100 μg mL$^{-1}$, 200 μg mL$^{-1}$, 500 μg mL$^{-1}$ equivalent to 2–1092 μM) of Hma, Hema, Hdpp, Hmpp, Ln(ma)$_3$, Ln(ema)$_3$, Ln(mpp)$_3$, and Ln(dpp)$_3$, Ln = La, Gd, Yb (dissolved in 1% DMSO/media solution, highest concentration of DMSO 100 μg mL$^{-1}$). After an incubation of 72 h, a 50 μL aliquot of MTT (2.5 mg mL$^{-1}$ in PBS) was added to each well of the plate. The plate was further incubated for 3 h at 37 °C during which time purple formazan crystals formed at the bottom of the wells. The solution of each well was carefully aspirated leaving the formazan crystals which were dissolved in DMSO (150 μL). The absorbance of each well was measured at 570 nm using a microplate reader (Spectra Max 190, Molecular Devices). Cell viability was calculated relative to the 100% control (DMSO plus media). The IC$_{50}$ was determined by plotting the percent cell viability *vs.* drug concentration (logarithmic scale) and finding the concentration at which 50% of the cells were viable relative to the control. Values are presented as means ± SD, based on ≥ 6 independent trials.

### Protein concentration

Total protein content was determined in lysed cells using the bicinchoninic acid protein assay (BCA™ Protein Assay Kit) from Pierce Biotechnology, Inc. (Rockford, IL, USA). After performing the cell uptake and bifunctional transport studies, the assay media was aspirated, cells were washed 3 times with PBS and were lysed. A BSA standard curve was constructed in the range of 25 μg mL$^{-1}$ to 2 mg mL$^{-1}$. Exactly 10 μL of both standards and cell samples (in triplicates) were aliquoted into a 96-well microtiter plate and 200 μL of Reagent (Mix A : B = 50 : 1) was added to each well. Absorbance was measured after 1 h at room temperature at 540 nm with a Multiscan Ascent Multi-plate reader from Labsystems. Protein concentration of each sample was determined against the standard curve.

### Caco-2 cell uptake studies

Caco-2 cells, passage number 25 to 30, were seeded at 5000 cells cm$^{-2}$ into 6-well plates and incubated in 37 °C in a humidified

atmosphere of 5% $CO_2$. The medium was changed every other day. After reaching 80% confluency, the cells were washed with PBS. The medium was removed and replaced with either fresh medium, or medium plus compound ($La(ma)_3$, $Gd(ma)_3$, $Yb(ma)_3$, $La(ema)_3$, $La(dpp)_3$, $La_2(CO_3)_3$) at concentrations of 100 μg $mL^{-1}$ (equivalent to 218–179 μM). The plate was incubated at 37 °C in a humidified atmosphere of 5% $CO_2$ for 4 h. Treatment solutions were aspirated and cells were washed three times with ice-cold PBS to remove any unbound $LnL_3$. Cells were lysed with 1 mL of lysis buffer (50 mM Hepes, 150 mM NaCl, 2 mM EDTA, 0.5% Na-deoxycholate, 1% NP-40) plus protease inhibitor cocktail (1 : 1000 dilution). The lysed cell solution was transferred into separate 1.5 mL Eppendorf tubes. Culture plate wells were rinsed with another 0.3 mL of lysis buffer, the combined cell/media samples were kept for later analysis by ICP-MS. The protein content was determined by a Pierce BCA assay using 10 μL of the lysed cells (vortexed thoroughly and pelleted by centrifugation at 12 000 rpm for 3 min). The concentrations are reported as % uptake of μM Ln(III) $mg^{-1}$ protein ± SD. Group values were compared by ANOVA with a Newman–Keuls post analysis. A $P$ value $< 0.05$ was considered to be statistically significant.

### Bifunctional transport assay

Caco-2 cells, passage number 30, were seeded at 5000 cells $cm^{-2}$ in polycarbonate membrane 12-well Transwell plates (Corning, Costar Corp.) and incubated at 37 °C in a humidified atmosphere of 5% $CO_2$. The media was changed every other day. Uptake studies were conducted when the TEER readings reached 400 Ω $cm^{-2}$. Prior to permeability studies, the cells were washed with PBS and the culture media was replaced with fresh media (control) or media plus compound (concentration of 100 μg $mL^{-1}$ for all tested compounds, equivalent to 218–179 μM, including $La(ma)_3$, $Gd(ma)_3$, $Yb(ma)_3$, $La(ema)_3$, $La(dpp)_3$, $La_2(CO_3)_3$) on the apical or basolateral side. The integrity of the Caco-2 cell monolayer was monitored by measuring the TEER values at each time point. The amount of permeated solute was determined by removing 100 μL aliquots from either the basolateral or apical side, opposite to the side on which the compound was added, at 10, 30, 60, 120, 180 and 240 min and replaced with fresh media. The plate was incubated at 37 °C in a humidified atmosphere of 5% $CO_2$ in between sample removal periods. All media was aspirated after 4 h, vacuum dried, and acid digested for further analysis. The cells were washed 3 times with PBS, the membrane was removed and lysed in 1 mL of 0.1 N NaOH. Exactly 10 μL of the lysed cells (vortexed thoroughly and pelleted by centrifugation at 12 000 rpm for 3 min) were analyzed for protein content using the Pierce BCA assay. The amount of Ln(III) ions accumulated in the cells, in addition to the concentration of Ln(III) ions in the apical or basolateral chambers were evaluated by ICP-MS. The % compound transported ± SD was determined by dividing the Ln(III) concentration found in either the basolateral or apical chamber by the total concentration of Ln(III) found in the study (concentration of Ln(III) in the apical and basolateral chambers, and in the cell membrane).

The apparent permeability ($P_{app}$, cm $s^{-1}$) coefficient from the bidirectional transport of the Ln(III) complexes were calculated using eqn (1):

$$P_{app} = (dQ/dt)/(AC_o) \quad (1)$$

where $dQ/dt$ (nmol $s^{-1}$) is the flux rate of mass transport across the monolayers, $A$ is the surface area of the insert membrane (1.13 $cm^2$), and $C_o$ is the initial concentration (μM) of the compound in the donor chamber. The flux rates were determined by plotting the concentration of Ln(III) ions determined by ICP-MS as a function of time, with the slope calculated *via* linear regression.

### Hydroxyapatite *in vitro* binding study

Samples containing exactly 20 mg of dried hydroxyapatite (HA, Sigma, St. Louis, MO, USA) were suspended in 2 mL of physiological 0.9% saline solution, pH 7.4 in 13 × 100 mm test tubes and incubated overnight at 37 °C to allow for equilibration of the samples. The metal complexes ($La(ma)_3$, $Eu(ma)_3$, $Gd(ma)_3$, $Tb(ma)_3$, $Yb(ma)_3$, $La(ema)_3$, $La(dpp)_3$, and $La_2(CO_3)_3$) were dissolved in DMSO, final concentration 5 mg $mL^{-1}$. Appropriate volumes of the DMSO solutions were added in order to achieve 1 μM concentration for all compounds tested (maximum concentration of DMSO in each sample ≤ 0.0005%) and the mixture was shaken gently. After incubation (5, 15 min, 3, and 24 h, 6 vials for each time point), the solution was centrifuged at 3200 rpm for 5 min. Supernatants were carefully removed and placed in 10 mL scintillation vials. Each pellet was washed twice with 1 mL of saline solution to remove any unbound metal ion from the pellet. The washings were collected after centrifugation and the supernatant was filtered through a 0.22 μm Millipore filter. Exactly 1 mL of the supernatant samples were vacuum centrifuged, dried overnight (excluding $Eu(ma)_3$ and $Tb(ma)_3$ samples) and resuspended in 2 mL of concentrated Seastar nitric acid for digestion (see later for procedure) and diluted accordingly for ICP-MS analysis. The remaining solution was used in determination of the free ligand content by UV-vis of appropriate dilutions. The $Eu(ma)_3$ and $Tb(ma)_3$ samples were used after filtering and diluted appropriately for fluorescence studies. The HA samples were dissolved in 2 mL of concentrated Seastar nitric acid, acid digested and diluted accordingly for ICP-MS analysis. The total amount of Ln(III) for each HA-binding experiment was determined by adding the Ln(III) concentration found in the supernatant with the concentration found in the HA samples. Percent HA-binding ± SD was determined by dividing the Ln(III) concentration from the HA sample by the total Ln(III) concentration found (HA and supernatant) for each sample. Group values were compared by ANOVA with Newman–Keuls post analysis. A $P$ value $< 0.05$ was considered to be statistically significant.

### Ln(III) analysis by ICP-MS

High resolution ICP-MS Thermo Finnigan Element2 was used to analyze the Ln(III) content of the cell lysates, solutions from both the apical and basolateral transport studies, and solutions and solid HA samples from the HA binding experiments. High purity standards ($In_2O_3$, $La_2O_3$, $Gd_2O_3$, and $Yb_2O_3$ 1000 μg $mL^{-1}$ in 2% $HNO_3$) were purchased from Delta Scientific Laboratory Products Ltd. (Spring City, PA). All materials used for the digestions of samples and for ICP-MS including glassware, Teflon boiling chips, sample holders, pipettes, and pipette tips were soaked in 2% Extran solution for 24 h, rinsed with deionized, distilled water, soaked overnight in 1% Seastar nitric acid, rinsed with deionized distilled

 

water, and finally left to dry in a dust-free environment prior to use. All samples were vacuum centrifuged to complete dryness and digested in acid using the following procedure before analysis. The redissolved digests were diluted accordingly with 1% nitric acid and their lanthanide contents analyzed by monitoring *m/z* 139, 158, and 174 for $^{139}$La, $^{158}$Gd, $^{174}$Yb, respectively. Samples were analyzed in the 'peak jump' mode and all signals corrected according to the internal $^{115}$In standard. Interference corrections for $^{158}$Gd were made by monitoring Dy at *m/z* 161.

### Acid digestion for ICP-MS analysis

Dried samples (vacuum centrifugation) were dissolved in 2 mL of Seastar concentrated nitric acid. Samples were transferred to test tubes with two or three Teflon boiling chips and placed in a block heater (Standard Heatblock, VWR Scientific Products). The temperature was slowly raised to 105 °C over 1 h and then maintained at 105 °C for 24 h. Approximately 2 mL of 30% hydrogen peroxide (Fisher Scientific) was added to each sample before heating at 140 °C for 24 h. The temperature was increased to 150 °C and samples were evaporated to dryness. Subsequently, samples were redissolved in 3 mL of 10% nitric acid and stored in 4 mL high density polyethylene bottles (Wheaton, Milville, NJ) at 4 °C.

### Ligand analysis by UV-Vis Assay

A calibration curve consisting of appropriate concentrations of dissolved ligand in 0.9% physiological saline solution was constructed for Hma, Hema and Hdpp at $\lambda_{max} = 273, 279, 275$ nm, respectively. The undigested supernatants from La(ma)$_3$, Eu(ma)$_3$, Gd(ma)$_3$, Tb(ma)$_3$, Yb(ma)$_3$ La(ema)$_3$, and La(dpp)$_3$–HA binding studies for all four time points were diluted 100 fold with 0.9% physiological saline solution. The concentration of ligand in solution was calculated by comparing the absorbances collected from the supernatant solutions to the previously constructed calibration curves. High concentration of the ligand in solution indicates dissociation of the $LnL_3$ complex upon HA binding. Percent ligand in solution was determined by dividing the ligand concentration determined in the supernatant by the total ligand concentration added.

### Eu(ma)$_3$ and Tb(ma)$_3$ analysis by fluorescence assay

A calibration curve over a range of concentrations was constructed by integrating the area under the most intense fluorescence peak ($\lambda_{em}$ = 641 for Tb(ma)$_3$ and 642 nm for the Eu(ma)$_3$) and plotted against the known concentration. Concentrations of the complexes in solution were determined by comparing their integrated area under the most intense fluorescence peak against the calibration curve. Percent Ln(III) bound was determined by subtracting the amount of Tb(III) or Eu(III) found in the supernatant from the total amount of Ln(III) added to the sample. This value was then divided by the total ligand concentration.

### Xylenol orange assay

Approximately 20 mg of proligand, HA, $LnL_3$, $Ln(NO_3)_3$, solid samples from the metal–HA binding studies as well as the supernatant from the same experiment were dissolved in minimal amounts of 6 M HCl. The pH was adjusted to 5 and diluted appropriately with an aqueous 20% hexamethylenetetramine buffer. Presence of free Ln(III) ions were confirmed by the immediate appearance of a red colour in the solution upon the addition of xylenol orange sodium salt.

## Acknowledgements

We thank Dr Elena Polishchuk and Candice Martins for help with MTT assays, Drs M. J. Abrams and G. J. Bridger for discussions, Dr W. R. Cullen and Vivian W.-M. Lai for their expertise in acid digestion technique and for the use of their equipment, and Bert Mueller for help with the ICP-MS. We acknowledge support from the Natural Sciences and Engineering Research Council of Canada and a University Graduate Fellowship (CAB) at the University of British Columbia.

## References

1 Government of Canada; http://www.biobasics.gc.ca/english/View.asp?x = 770, (accessed Jan. 11, 2007).
2 K. F. Mauck and B. L. Clarke, *Mayo Clin. Proc.*, 2006, **81**, 662.
3 D. W. Dempster and R. Lindsay, *Lancet*, 1993, **341**, 797.
4 M. T. McDermott, C. Zapalowski and P. D. Miller, *Osteoporosis*, Hanley & Belfus, Toronto, ON, 2004, p 1-168.
5 J. N. Fordham, *Osteoporosis*, Churchill Livingstone, Toronto, 2004, p 223.
6 M. A. Karsdal and C. Christiansen, *Future Rheum.*, 2006, **1**, 683.
7 P. J. Marie, *Bone*, 2006, **38**, S10.
8 S. C. Verberckmoes, M. E. D. Broe and P. C. D'Haese, *Kidney Int.*, 2003, **64**, 534.
9 E. Pidcock and G. R. Moore, *J. Biol. Inorg. Chem.*, 2001, **6**, 479.
10 T. J. Webster, E. A. Massa-Schlueter, J. L. Smith and E. B. Slamovich, *Biomaterials*, 2004, **25**, 2111.
11 D. Nigel, W. Joseph and D. Michael, *World Patent, WO 02/00227 A2*, 2002.
12 P. Caravan, J. J. Ellison, T. J. McMurry and R. B. Lauffer, *Chem. Rev.*, 1999, **99**, 2293.
13 I. Kostova, *Curr. Med. Chem.*, 2005, **5**, 591.
14 N. Sabbatini, M. Guardigli and J.-M. Lehn, *Coord. Chem. Rev.*, 1993, **123**, 201.
15 S. P. Fricker, *Chem. Soc. Rev.*, 2006, **35**, 524.
16 D. Nayak and S. Lahiri, *J. Radioanal. Nucl. Chem.*, 1999, **242**, 423.
17 W. A. Volkert and T. J. Hoffman, *Chem. Rev.*, 1999, **99**, 2269.
18 M. A. Santos, M. Gil, L. Gano and S. Chaves, *J. Biol. Inorg. Chem.*, 2005, **10**, 564.
19 M. A. Santos, S. Gama, L. Gano, G. Cantinho and E. Farkas, *Dalton Trans.*, 2004, 3772.
20 D. M. J. Doble, M. Melchior, B. O'Sullivan, C. Sierring, J. Xu, V. C. Pierre and K. N. Raymond, *Inorg. Chem.*, 2003, **42**, 4930.
21 M. M. Jones, J. J. Molenda, T. P. Hanusa and M. W. Voehler, *J. Inorg. Biochem.*, 1996, **62**, 127.
22 A. E. V. Gordon, J. Xu, K. N. Raymond and P. W. Durbin, *Chem. Rev.*, 2003, **103**, 4207.
23 K. H. Thompson, C. A. Barta and C. Orvig, *Chem. Soc. Rev.*, 2006, **35**, 545.
24 R. C. Hider and T. Zhou, *Ann. N. Y. Acad. Sci.*, 2005, **1054**, 141.
25 Z. D. Liu and R. C. Hider, *Med. Res. Rev.*, 2002, **22**, 26.
26 R. A. Yokel, *Coord. Chem. Rev.*, 2002, **228**, 97.
27 M. A. Santos, *Coord. Chem. Rev.*, 2002, **228**, 187.
28 Titan Pharmaceuticals Inc., http://www.titanpharm.com/pt-gallium.html, (accessed Jan 2006).
29 D. J. Clevette and C. Orvig, *Polyhedron*, 1990, **9**, 151.
30 Z. Zhang, D. M. Lyster, G. A. Webb and C. Orvig, *Nucl. Med. Biol.*, 1992, **19**, 327.
31 D. E. Green, C. L. Ferreira, R. V. Stick, B. O. Patrick, M. J. Adam and C. Orvig, *Bioconjugate Chem.*, 2005, **16**, 1597.
32 M. A. Barrand, B. A. Callingham and R. C. Hider, *J. Pharm. Pharmacol.*, 1987, **39**, 203.
33 M. A. Barrand, R. C. Hider and B. A. Callingham, *J. Pharm. Pharmacol.*, 1990, **42**, 279.

34 D. G. Maxton, R. P. H. Thompson and R. C. Hider, *J. Nutr.*, 1994, **71**, 203.
35 K. H. Thompson, J. H. McNeill and C. Orvig, *Chem. Rev.*, 1999, **99**, 2561.
36 K. N. Raymond and V. C. Pierre, *Bioconjugate Chem.*, 2005, **16**, 3.
37 L. F. Cavalieri, *Chem. Rev.*, 1947, **4**, 525.
38 R. L. N. Harris, *Aust. J. Chem.*, 1976, **29**, 1329.
39 N. K. Dutt and U. U. M. Sarma, *J. Inorg. Nucl. Chem.*, 1975, **37**, 1801.
40 S. Ahmed, J. Burgess, B. Hurman and S. A. Parsons, *Polyhedron*, 1994, **13**, 23.
41 D. Fregona, G. Faraglia, R. Graziani, U. Casellato and S. Sitran, *Gazz. Chim. Ital.*, 1994, **124**, 153.
42 J. Fogh, J. M. Fogh and T. Orfeo, *J. Natl. Cancer Inst.*, 1977, **59**, 221.
43 M. N. Garcia-Casal, I. Leets and M. Layrisse, *J. Nutr.*, 2000, **130**, 5.
44 J. F. Vanchon and P. Beaulieu, *Gastroenterology*, 1992, **103**, 414.
45 Z. Zhang, S. J. Rettig and C. Orvig, *Inorg. Chem.*, 1991, **30**, 509.
46 V. Monga, B. O. Patrick and C. Orvig, *Inorg. Chem.*, 2004, **44**, 2666.
47 M. M. Finnegan, T. G. Lutz, W. O. Nelson, A. Smith and C. Orvig, *Inorg. Chem.*, 1987, **26**, 2171.
48 W. O. Nelson, T. B. Karpishin, S. J. Rettig and C. Orvig, *Can. J. Chem.*, 1987, **66**, 123.
49 G. Faraglia, D. Fregona and S. Sitran, *Main Group Met. Chem.*, 1994, **17**, 649.
50 D. J. Clevette, D. M. Lyster, W. O. Nelson, T. Rihela, G. A. Webb and C. Orvig, *Inorg. Chem.*, 1990, **29**, 667.
51 C. Tedeshi, J. Azema, H. Gornitzka, P. Tisnes and C. Picard, *Dalton Trans.*, 2003, 1738.
52 E. C. Alyea, A. Malek and A. E. Vougioukas, *Can. J. Chem.*, 1981, **60**, 667.
53 L. M. Brown and K. S. Mazdiuasni, *Inorg. Chem.*, 1970, **9**, 2783.
54 W. O. Nelson, T. B. Karpishin, S. J. Rettig and C. Orvig, *Inorg. Chem.*, 1988, **27**, 1045.
55 N. Sabbatini and M. Guardigli, *Coord. Chem. Rev.*, 1993, **123**, 201.
56 G. R. Choppin and D. R. Peterman, *Coord. Chem. Rev.*, 1998, **174**, 283.
57 S. I. Weissman, *J. Chem. Phys.*, 1942, **10**, 214.
58 X.-P. Yang, B.-S. Kang, W.-K. Wong, C.-Y. Su and H.-Q. Liu, *Inorg. Chem.*, 2003, **42**, 169.
59 W. D. Kim, G. E. Kiefer, F. Maton, K. McMillan, R. N. Muller and A. D. Sherry, *Inorg. Chem.*, 1995, **34**, 2233.
60 L. Tei, A. J. Blake, M. W. George, J. A. Weinstein, C. Wilson and M. Schroder, *Dalton Trans.*, 2003, 1693.
61 A. F. Kirby, D. Foster and F. S. Richardson, *Chem. Phys. Lett.*, 1983, **95**, 507.
62 A. F. Kirby and F. S. Richardson, *J. Phys. Chem.*, 1983, **87**, 2544.
63 S. J. P. Damment and M. Gill, *J. Am. Soc. Nephrol.*, 2003, **14**, FP0653.
64 A. W. K. Ng, T. Lukic, H. P. Pritchard and K. M. Wasan, *Cardiovasc. Drug Rev.*, 2003, **21**, 151.
65 M. Yazdanian, S. L. Glynn, J. L. Wright and A. Hawi, *Pharmacol. Res.*, 1998, **15**, 1490.
66 H. Okhee, M. L. Failla, D. Hill, E. R. Morris and J. J. C. Smith, *J. Nutr.*, 1994, **124**, 580.
67 V. D. Makhey, A. Guo, D. A. Norris, P. Hu, J. Yan and P. J. Sinko, *Pharmacol. Res.*, 1998, **15**, 1160.
68 V. Risovic, K. Sachs-Barrable, M. Boyd and K. M. Wasan, *Drug Dev. Ind. Pharm.*, 2004, **30**, 767.
69 M. Ochsenkuhn-Petropoulou, K. Ochsenkuhn and J. Luck, *Spectrochim. Acta, Part B*, 1991, **46**, 51.
70 T. Mosmann, *J. Immunol. Methods*, 1983, **65**, 55.
71 E. van Niekerk, J. F. O'Sullivan, G. K. Joone and C. E. J. van Rensburg, *Invest. New Drugs*, 2001, **19**, 211.
72 X.-P. Huang, M. Spino and J. J. Thiessen, *Pharmacol. Res.*, 2006, **23**, 280.
73 M. A. Santos, S. Gama, L. Gano, G. Cantinho and E. Farkas, *Coord. Chem. Rev.*, 2002, **228**, 187.
74 F. C. Alves, P. Donato, A. D. Sherry, A. Zaheer, S. Zhang, A. J. M. Lubag, M. E. Merritt, R. E. Lenkinski, J. V. Frangioni, M. Neves, M. I. M. Prata, A. C. Santos, J. J. P. de Lima and C. F. G. C. Geraldes, *Invest. Radiol.*, 2003, **38**, 750.
75 L. Yu, D. Chen, J. Li and P. G. Wang, *J. Org. Chem.*, 1997, **62**, 3575.
76 J. Rudovsky, M. Botta, P. Hermann, A. Koridze and S. Aime, *Dalton Trans.*, 2006, 2323.
77 M. Wakamura, K. Kandori and T. Ishikawa, *Colloids Surf., A*, 2000, **164**, 297.
78 A. Lebugle, F. Pelle, C. Charvillat, I. Rousselot and J. Y. Chane-Ching, *Chem. Commun.*, 2006, 606.
79 D. Choi and P. Kumta, *J. Am. Ceram. Soc.*, 2006, **89**, 444.
80 M. C. Chang and J. Tanaka, *Biomaterials*, 2002, **23**, 4811.
81 M. E. Fleet and X. Liu, *J. Solid State Chem.*, 2000, **149**, 391.




 